

Paléo-océanographie  
Paléoclimatologie  
Isotopes  
Salinité  
Atlantique

Paleo-oceanography  
Paleoclimatology  
Isotopes  
Salinity  
Atlantic Ocean

# Surface salinity reconstruction of the North Atlantic Ocean during the last glacial maximum

Jean-Claude DUPLESSY <sup>a</sup>, Laurent LABEYRIE <sup>a</sup>, Anne JUILLET-LECLERC <sup>a</sup>, Florence MAITRE <sup>a</sup>, Josette DUPRAT <sup>b</sup>, Michael SARNTHEIN <sup>c</sup>

<sup>a</sup> Centre des Faibles Radioactivités, Laboratoire mixte CNRS-CEA, 91198 Gif-sur-Yvette Cedex, France.

<sup>b</sup> Département de Géologie et Océanographie, Université de Bordeaux-1, avenue des Facultés, 33405 Talence Cedex, France.

<sup>c</sup> Geologisch-Paläontologisches Institut, Universität Kiel, Olshausenstrasse 40/60, 2300-Kiel, Germany.

Received 5/02/91, in revised form 28/03/91, accepted 4/04/91.

## ABSTRACT

We have developed a new method to reconstruct surface water salinity of the North Atlantic Ocean, based on a comparison between transfer function estimates of sea surface temperature and the oxygen isotope ratio of two common planktonic foraminiferal species, *N. pachyderma* (left coiling) and *G. bulloides*. We first used core-top analyses to demonstrate that, under modern conditions, the paleotemperatures determined from the isotopic composition of foraminiferal shells are linearly linked to the summer sea surface temperature only within a certain temperature range, characteristic of each species, which is termed the "optimum temperature range". We then used this information to derive an estimate of the isotopic composition and salinity of the North Atlantic surface water during the last glacial maximum. The resulting reconstruction shows the presence of a sharp salinity gradient associated with the polar front. However, high-salinity water was present near 30-40°W, north of the polar front. This pattern would have provided the flux of salt required for increasing the density of surface water during winter and its subsequent sinking to the abyss.

*Oceanologica Acta*, 1991. 14, 4, 311-324.

## RÉSUMÉ

Reconstitution de la salinité des eaux de surface de l'Océan Atlantique Nord au cours du dernier maximum glaciaire

Nous avons développé une nouvelle méthode permettant de reconstruire la salinité de l'eau de surface de l'Océan Atlantique Nord dans le passé. Celle-ci repose sur la comparaison de l'estimation de température des eaux superficielles avec la composition isotopique de l'oxygène des foraminifères planctoniques *N. pachyderma* et *G. bulloides* qui ont vécu dans cette eau. Dans un premier temps, nous démontrons, par l'analyse de sommets de carottes représentant les conditions actuelles, que les paléotempératures isotopiques sont linéairement liées aux températures d'été des eaux de surface, mais uniquement dans une gamme de température, caractéristique de chaque espèce, et que nous appelons le domaine optimal de température de l'espèce. Dans un second temps, nous

supposons que ce domaine optimal de température est resté constant dans le passé, et nous utilisons la calibration réalisée sur les conditions actuelles pour estimer la composition isotopique de l'oxygène et la salinité de l'eau de surface de l'Océan Atlantique Nord pendant le dernier maximum glaciaire. La reconstruction obtenue montre la présence d'un fort gradient de salinité associé au front polaire. Toutefois, la présence d'eau de salinité élevée vers 30-40°W au nord du front polaire, témoigne de l'existence d'un flux de sel vers les hautes latitudes, qui devait faciliter les formations d'eau profonde pendant les conditions hivernales.

*Oceanologica Acta*, 1991, **14**, 4, 311-324.

## INTRODUCTION

Oceanic circulation is driven by the wind field at the sea surface and the density of the water. In order to obtain a complete reconstruction of the ocean in the geological past, it is therefore necessary to estimate both the temperature and the salinity of the various water masses. Sea-surface temperature can be estimated by planktonic fauna analysis (Imbrie and Kipp, 1971) and a global reconstruction of the sea-surface temperature at the last glacial maximum (LGM) has been obtained by CLIMAP (1976; 1981). A similar reconstruction for the sea surface salinity, based on empirical transfer functions, is not available because the salinity of surface water is not independent of the temperature. Evaporation is stronger in warm areas, whereas precipitation dominates in cold areas. Both processes result in a net transport of freshwater from the warm surface ocean to the cold surface ocean via the atmosphere. As a consequence, the salinity of surface waters decreases from the tropics to the high latitudes and bears a rough linear correlation to temperature (Fig. 1). The statistical analysis of planktonic faunal variations depicts primarily temperature variations. Surface salinity estimates can only be obtained when surface waters exhibit large salinity gradients and small temperature gradients, for instance in the Northern Indian Ocean (Cullen, 1981).

Another possible approach to estimate past salinity relies on oxygen isotope analysis. Polar water has lower  $\delta^{18}\text{O}/\delta^{16}\text{O}$

ratios than do tropical and temperate waters. These differences are closely tied to the ocean surface salinity distribution (Epstein and Mayeda, 1953; Craig and Gordon, 1965; Duplessy, 1970); the higher the salinity, the higher the  $\delta^{18}\text{O}/\delta^{16}\text{O}$  ratio (Fig. 2). Excess evaporation concentrates the less volatile  $\text{H}_2^{18}\text{O}$  together with salt, while precipitation, more depleted in  $\text{H}_2^{18}\text{O}$  than ocean water, decreases both salinity and the  $\delta^{18}\text{O}/\delta^{16}\text{O}$  ratio of the sea surface water. The  $\delta^{18}\text{O}/\delta^{16}\text{O}$  ratio of planktonic foraminifera records these variations since it depends on both the  $\delta^{18}\text{O}/\delta^{16}\text{O}$  ratio and the temperature of the sea water in which foraminifera have grown : on the one hand, the  $\delta^{18}\text{O}/\delta^{16}\text{O}$  ratio of  $\text{CaCO}_3$  directly reflects variations of the  $\delta^{18}\text{O}/\delta^{16}\text{O}$  ratio of the ambient water; on the other hand, the oxygen isotope fractionation between  $\text{CaCO}_3$  and water increases by about 0.25 ‰ for each degree the water is cooled (Epstein *et al.*, 1953; Shackleton, 1974). This is expressed by the paleotemperature equation :

$$T = 16.9 - 4.38 \times (\delta^{18}\text{O}_{\text{carbonate}} - \delta^{18}\text{O}_{\text{water}}) + 0.10 \times (\delta^{18}\text{O}_{\text{carbonate}} - \delta^{18}\text{O}_{\text{water}})^2$$

This equation was first tentatively used to determine quantitatively the range of oceanic temperature fluctuations in the Quaternary (Emiliani, 1955). In contrast, if the temperature of deposition of foraminiferal calcite is known (for instance through a transfer function estimate), it becomes feasible to calculate the  $\delta^{18}\text{O}/\delta^{16}\text{O}$  of the water in which the foraminifera have grown. Only a few attempts have been made to use stable isotope analysis of planktonic forami-

GEOSECS Atlantic Surface Waters (0-250m)

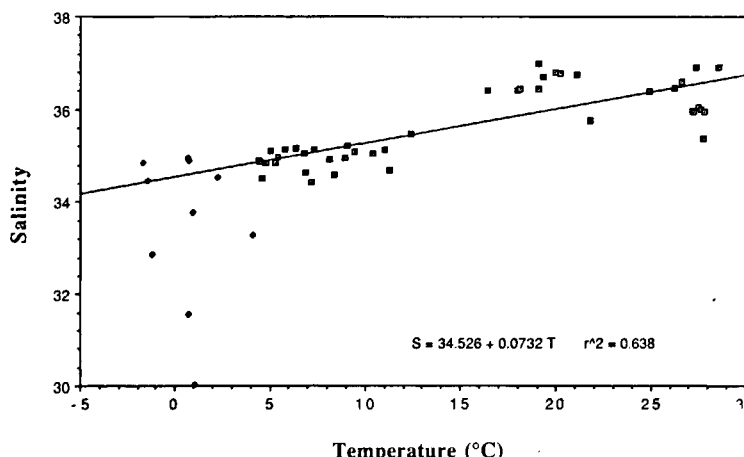


Figure 1

Plot of the salinity against temperature for waters collected in the upper 250 m of Atlantic Ocean during the GEOSECS expedition (GEOSECS, 1987). Values corresponding to temperatures < 4.5°C, possibly contaminated by local freshwater inflow or ice melting, have been excluded from the regression.

Variations, en fonction de la température, de la salinité des eaux collectées dans la couche superficielle (les 250 premiers mètres) de l'Océan Atlantique Nord au cours des campagnes GEOSECS (GEOSECS, 1987). Pour les températures < 4,5°C, les eaux pouvaient être contaminées par des apports locaux d'eau douce, et ont été exclues de la régression.

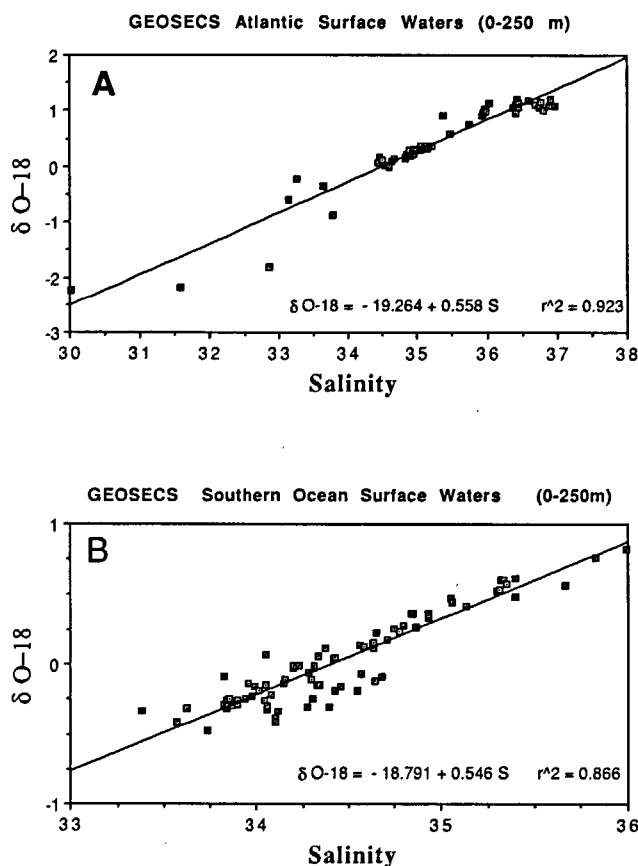


Figure 2

Plot of the  $\delta^{18}\text{O}$  value against salinity for waters collected in the upper 250 m of Atlantic (A) and Southern (B) oceans during the GEOSECS expedition (GEOSECS, 1987).

Variations, en fonction de la salinité, de la composition isotopique de l'oxygène ( $\delta^{18}\text{O}$ ) des eaux collectées dans la couche superficielle (les 250 premiers mètres) de l'Océan Atlantique (A) et de l'Océan Austral (B), au cours des campagnes GEOSECS (GEOSECS, 1987).

nifera to estimate past surface salinity (e.g. Fillon and Williams, 1984), because the comparison of planktonic foraminifera  $^{18}\text{O}/^{16}\text{O}$  variations and sea surface temperature (SST) changes estimated by faunal analysis showed that no individual species of planktonic foraminifera records the whole range of temperature changes (Bard *et al.*, 1987). This is interpreted as an indication that individual species of planktonic foraminifera have specific temperature tolerance ranges (Bé, 1960). Sediment trap studies have shown that various species of planktonic foraminifera in a given oceanic basin exhibit a seasonal succession (Reynolds-Sautter and Thunell, 1989), suggesting that thermal conditions in the euphotic zone control both the vertical distribution and life season of these zooplankton (Thunell and Honjo, 1987; Wefer *et al.*, 1987; 1988). This hypothesis is supported by stable isotope analysis (Fairbanks and Wiebe, 1980; Keigwin and Boyle, 1989; Charles and Fairbanks, 1990; Bard *et al.*, 1989).

In this paper, we present an attempt to estimate the range of sea surface temperatures for which the  $^{18}\text{O}/^{16}\text{O}$  ratios of *Neogloboquadrina pachyderma* and *Globigerina*

*bulloides*, two species common in the North Atlantic, are related to the summer sea-surface water temperature (SST) and the ambient  $^{18}\text{O}/^{16}\text{O}$  ratio. We use measurements performed in different laboratories. However the Bergen, Cambridge, Gif and Kiel laboratories, which constitute the major sources of data, are closely intercalibrated. This effort allows us to compare data with minimal error. We then use this information to compare summer SST estimates obtained by CLIMAP (1981) with  $^{18}\text{O}/^{16}\text{O}$  measurements made on planktonic foraminifera from North Atlantic cores to derive estimates of the surface water  $^{18}\text{O}/^{16}\text{O}$  ratio and salinity during the maximum of the last glaciation. All the isotope measurements are reported using the conventional  $\delta^{18}\text{O}$  notation, the standards being PDB for the carbonates and SMOW for the water.

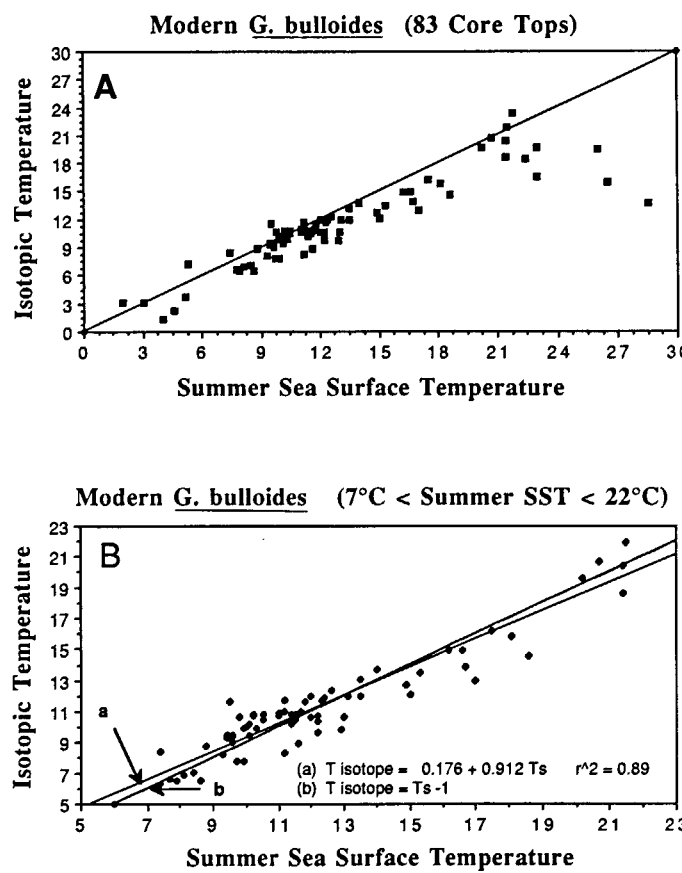


Figure 3

A: Plot of the isotopic temperature calculated from *G. bulloides*  $\delta^{18}\text{O}$  values against summer sea surface temperature for 83 core tops from the North Atlantic and the Southern Ocean.

B: Comparison of the regression line (a) calculated for samples for which the summer SST is in the range 7-22°C, with the linear relationship (b):  $T_{\text{isotope}} = \text{summer SST} - 1^\circ\text{C}$ .

A : Variations, en fonction de la température d'été des eaux superficielles, de la température isotopique calculée à partir de la composition isotopique ( $\delta^{18}\text{O}$ ) de *G. bulloides*. 83 sommets de carottes provenant de l'Océan Atlantique Nord et de l'Océan Austral ont été utilisés.

B : Comparaison de la droite de régression (a), calculée pour les échantillons provenant de carottes pour lesquelles la température d'été des eaux de surface est comprise entre 7 et 22°C, avec la droite (b) d'équation :  $T_{\text{isotope}} = \text{température d'été des eaux superficielles} - 1^\circ\text{C}$ .

Table 1

*Summary of the data used for the calibration of the oxygen isotopic ratio of Globigerina bulloides.*

*Latitudes and longitudes are expressed as degrees and minutes. Positive values for latitude and longitude indicate N and E. Negative values indicate S and W. The sea surface delta O-18 values have been calculated using the regression lines of Figure 2. Summer sea surface temperature and salinity are from Levitus (1982).*

*Data Source : D = Durazzi (1981) ; W & S = Winn and Sarnthein, unpublished ; T. J. = Truls Johannessen Thesis data (1987) corrected by +0.16 (pers. comm., 1988) ; Zahn = Zahn thesis (1986) ; Gif = analysis made at Gif for this work.*

Données utilisées pour la calibration de la composition isotopique de l'oxygène de *Globigerina bulloides*.

Les latitudes et longitudes sont exprimées en degrés et minutes ; les valeurs positives indiquent respectivement le Nord et l'Est, les valeurs négatives le Sud et l'Ouest. La température et la salinité des eaux de surface sont extraites de l'atlas de Levitus (1982). La composition isotopique de l'oxygène ( $\delta^{18}\text{O}$ ) des eaux superficielles a été calculée à partir des droites de régression des figures 2A et 2B.

Sources des données : D = Durazzi (1981) ; W & S = Winn et Sarnthein, données non publiées ; T. J. = thèse de Truls Johannessen (1987), données isotopiques corrigées de +0,16 ‰ (comm. pers., 1988) ; Zahn = thèse de R. Zahn (1986) ; Gif = analyses faites à Gif pour ce travail.

Core	Latitude	Longitude	$\delta^{18}\text{O}$ <i>G. bulloides</i>	Summer sea surface salinity	Calculated sea surface $\delta^{18}\text{O}$	Summer sea surface temperature	Isotopic temperature	Data source
V 28-29	72.11	- 5.16	2.09	34.6	0.05	5.3	7.3	D
V 28-30	71.10	- 1.37	2.15	35.2	0.38	7.4	8.4	D
V 28-41	67.41	5.00	1.42	35.3	0.44	9.5	11.6	D
57-12	67.04	- 7.18	2.45	34.9	0.21	7.7	6.6	T. J.
57-13	67.02	- 6.35	2.51	35	0.27	7.9	6.5	T. J.
57-14	66.59	- 6.12	2.37	35	0.27	8.4	7.1	T. J.
49-18	66.36	1.33	1.70	35.2	0.38	10.1	10.2	T. J.
49-20	66.36	2.39	1.77	35.2	0.38	10.3	9.9	T. J.
49-15	66.20	- 0.21	1.78	35.2	0.38	9.9	9.9	T. J.
52-41	65.36	- 4.37	1.81	35.1	0.33	9.4	9.5	T. J.
49-13	65.25	- 4.44	1.87	35.1	0.33	9.4	9.3	T. J.
49-14	65.25	- 3.13	1.83	35.1	0.33	9.6	9.4	T. J.
16130	65.06	- 2.24	1.61	35.2	0.38	9.8	10.6	T. J.
V 28-34	64.50	- 3.35	1.87	35.2	0.38	9.6	9.5	D
16132	64.33	- 0.43	1.54	35.2	0.38	10.5	10.8	T. J.
16136	64.00	- 0.43	1.62	35.2	0.38	10.5	10.5	T. J.
52-28	63.59	- 12.05	1.69	35.1	0.33	10	10.0	T. J.
16141	63.45	1.23	1.47	35.1	0.33	11.0	10.9	T. J.
49-39	63.27	3.02	1.34	34.8	0.16	11.6	10.8	T. J.
52-24	63.21	- 13.18	1.51	35.1	0.33	10.2	10.7	T. J.
16142	63.15	2.36	1.16	34.9	0.21	11.2	11.7	T. J.
16144	63.04	2.59	1.33	34.9	0.21	11.2	11.0	T. J.
49-08	63.03	0.47	1.48	35.0	0.27	12.0	10.6	T. J.
V 27-34	63.01	- 31.00	1.93	35.0	0.27	8.8	8.8	D
58-02	62.53	1.22	1.58	35	0.27	11.4	10.2	T. J.
58-03	62.53	1.22	1.57	35	0.27	11.4	10.3	T. J.
49-43	62.46	3.53	1.28	34.7	0.10	11.5	10.8	T. J.
57-20	62.39	1.4	1.43	35	0.27	11.4	10.8	T. J.
58-08	62.37	1.11	1.43	35	0.27	11.4	10.8	T. J.
V 27-36	62.27	- 19.30	1.56	35.1	0.33	11.5	10.5	D
NO 77-14	62.27	- 20.25	2.01	35.2	0.38	11.6	8.9	Gif
52-15	61.37	- 16.29	1.56	35.3	0.44	11.7	11.0	T. J.
V 27-38	61.22	- 11.29	2.22	35.3	0.44	11.2	8.3	D
52-04	61.21	- 3.12	1.26	35.2	0.38	12.0	12.0	T. J.
52-44	60.41	2.42	1.42	34.8	0.16	12.2	10.4	T. J.
52-54	60.33	2.51	1.61	34.8	0.16	12.2	9.7	T. J.
52-62	60.26	2.51	1.35	34.8	0.16	12.2	10.7	T. J.
52-14	60.24	- 12.25	1.41	35.3	0.44	11.8	11.6	T. J.
52-09	60.05	- 7.08	1.34	35.2	0.38	12.3	11.7	T. J.
52-13	59.39	- 9.18	1.25	35.3	0.44	12.6	12.3	T. J.
V 30-126	58.34	- 35.30	1.50	35.1	0.33	10.2	10.8	D
CH 73-108	58.05	- 10.43	1.35	35.3	0.44	12.4	11.9	D
V 27-110	56.54	- 18.50	1.31	35.3	0.44	13.1	12.0	D
V 30-122	56.48	- 38.30	1.65	34.8	0.16	10.1	9.5	D
V 30-124	56.44	- 42.30	1.72	34.7	0.10	9.6	9.0	D
V 23-23	56.04	- 44.33	2.02	34.7	0.10	9.7	7.8	D
V 27-111	56.04	- 24.30	1.73	35.1	0.33	12.9	9.8	D
CH73-136	55.34	- 14.28	1.37	35.4	0.49	13.5	12.0	Gif
NA 87-25	55.34	- 14.45	1.12	35.4	0.49	13.5	13.1	Gif
V 30-118	55.25	- 44.30	2.03	34.7	0.10	9.9	7.8	D
CH 73-139c	54.38	- 16.21	0.97	35.4	0.49	14.0	13.7	Gif
V 30-116	53.38	- 44.30	1.19	34.5	- 0.01	11.0	10.7	D
CH 73-141	52.52	- 16.31	1.21	35.4	0.49	14.9	12.7	Gif
M 17-045	52.26	- 16.40	1.02	35.4	0.49	15.3	13.5	W & S

Table 1 (cont.)

Core	Latitude	Longitude	$\delta^{18}\text{O}$ <i>G. bulloides</i>	Summer sea surface salinity	Calculated sea surface $\delta^{18}\text{O}$	Summer sea surface temperature	Isotopic temperature	Data source
V 27-19	52.06	- 38.48	1.33	34.7	0.10	13.0	10.6	D
V 27-17	50.05	- 37.18	1.12	35.0	0.27	15.0	12.1	D
V 29-183	49.08	- 25.30	0.75	35.5	0.55	16.2	14.9	D
CH 73-145	49.08	- 17.46	1.03	35.6	0.60	16.7	13.9	Gif
CH 73-147b	48.12	- 15.55	1.24	35.6	0.60	17.0	13.0	Gif
CH 72-101	47.28	- 8.34	0.73	35.5	0.55	16.6	14.9	Gif
NO 79-25	46.59	- 27.17	0.56	35.7	0.66	17.5	16.2	Gif
NO 79-29	46.18	- 15.04	0.68	35.8	0.69	18.1	15.8	Gif
SU 81-32	42.06	- 9.47	0.98	35.8	0.72	18.6	14.6	Gif
SU 81-18	37.46	- 10.11	0.00	36.1	0.88	20.2	19.6	Gif
SU 81-14	36.46	- 9.51	- 0.12	36.3	1.00	20.7	20.7	Gif
V 24-1	36.30	- 73.30	0.94	36.3	1.00	26.5	16.0	D
M 16-004	29.59	- 18.38	0.35	36.3	1.00	21.4	18.6	Zahn
M 16-006	29.14	- 11.29	- 0.63	36.4	1.05	21.8	23.3	Zahn
M 12-309	26.50	- 15.07	0.11	36.6	1.16	21.4	20.4	Zahn
M 12-392	25.10	- 16.51	- 0.22	36.6	1.16	21.5	21.9	Zahn
M 16-017	21.15	- 17.48	0.07	36.2	0.94	23.0	19.6	Zahn
M 16-030	21.14	- 18.03	0.73	36.2	0.94	23.0	16.6	Zahn
M 12-328	21.09	- 18.34	0.32	36.2	0.94	22.4	18.4	Zahn
M 13-289	18.04	- 18.01	- 0.13	35.8	0.72	26.0	19.5	Zahn
RC 10-49	16.34	- 79.31	1.24	35.9	0.77	28.5	13.7	D
<b>Southern Ocean</b>								
MD 80-304	- 51.04	67.44	3.10	33.9	- 0.29	4.6	2.2	Gif
MD 84-551	- 55.00	73.17	2.86	33.9	- 0.29	2.0	3.1	Gif
MD 88-770	- 46.01	96.28	1.91	34.0	- 0.24	8.1	6.9	Gif
KR MD 88-02	- 45.45	82.56	1.91	34.6	0.09	9.3	8.2	Gif
KR MD 88-05	- 52.57	109.55	2.87	33.9	- 0.29	3.0	3.1	Gif
KR MD 88-06	- 49.01	128.46	2.23	34.4	- 0.02	8.6	6.5	Gif
KR MD 88-10	- 54.11	144.48	2.65	33.8	- 0.35	5.1	3.7	Gif
KR MD 88-13	- 57.57	144.35	3.30	33.8	- 0.35	4.0	1.3	Gif

#### ISOTOPIC CALIBRATION OF *G. BULLOIDES* AND *N. PACHYDERMA*

We performed  $\delta^{18}\text{O}$  measurements on *G. bulloides* ( $> 150 \mu\text{m}$ ) from 83 core tops distributed throughout the North Atlantic Ocean and the Southern Ocean (excluding marginal basins, which exhibit large seasonal temperature/salinity variations during the year). Most of these cores had an isotope record long enough to confirm that upper Holocene levels were well-represented. The isotopic temperatures calculated according to the paleotemperature scale of Epstein *et al.* (1953) revised by Shackleton (1974), are reported in Table 1. As *G. bulloides* is considered to prefer warm conditions when a strong thermocline exists (Reynolds-Sautter and Thunell, 1989), the  $\delta^{18}\text{O}$  values for surface sea water ( $\delta\text{w}$ ) were calculated from summer salinity data gathered in the Levitus atlas (1982) and by applying the  $\delta\text{w}/\text{salinity}$  relationship derived from the GEOSECS data for the North Atlantic Ocean (Fig. 2A) and the Southern Ocean (Fig. 2B). We can neglect the fact that the  $\delta^{18}\text{O}/\text{salinity}$  relationship varies slightly from latitude to latitude (Craig and Gordon, 1965), because this introduces only minor changes in the  $\delta^{18}\text{O}$  estimates. The comparison of the Levitus summer SST with that derived from the isotopic measurements (Fig. 3A) shows several features already observed by Bard *et al.* (1989): isotopic temperatures derived from the  $\delta^{18}\text{O}$  values of *G. bulloides* covary with the summer SST only in the range 7 to 22°C,

which we shall call the "optimal temperature range" for this species. Outside of this range, in warm areas ( $T > 22^\circ\text{C}$ ), *G. bulloides* exhibits rather constant values and isotopic temperatures are significantly lower than atlas values, suggesting either that *G. bulloides* migrated into these regions only during cold years or lived preferentially in high productivity waters, which occur in lower latitudes during winter (Ganssen and Sarnthein, 1983). In cold areas ( $T < 7^\circ\text{C}$ ), *G. bulloides* is rare and the  $\delta^{18}\text{O}$  values exhibit a noticeable scatter. We can therefore derive paleoenvironmental information only when the foraminifera did not live under stressed conditions, *i.e.* when the summer SST was in the "optimal temperature range" of this species. Figure 3A also shows that the isotopic temperature of *G. bulloides* is generally lower than the summer SST. This is not a surprising result since the plankton bloom in the North Atlantic begins during the spring and lasts for several weeks. Also modern *G. bulloides* lives near the chlorophyll maximum, *i.e.* at temperatures slightly lower than those at the surface (Ganssen and Sarnthein, 1983). The assemblage from the sediment integrates the SST variations during the whole period of production of this individual species. A statistical analysis performed on core tops raised from locations where the summer SST is in the range 7 to 22°C shows that the isotopic temperature given by *G. bulloides* is highly correlated with the summer SST ( $r^2 = 0.89$ ) and that the slope of the regression line (0.91 with  $\sigma = 0.04$ ) is not significantly different from 1 at the  $2\sigma$  level. Over the whole "optimal temperature range" of

Table 2

*Summary of the data used for the calibration of the oxygen isotopic ratio of N. pachyderma (left coiling).*

*Latitudes and longitudes are expressed as degrees and minutes. Positive values for latitude and longitude indicate N and E. Negative values indicate S and W. The sea surface delta O-18 values have been calculated using the regression lines of Figure 2. Summer sea surface temperature and salinity are from Levitus (1982).*

*Data source : D = Durazzi (1981); M & F = Mix and Fairbanks (1985); KDS = Kellogg *et al.* (1978); Gif = analysis made at Gif for this work; J & V = Jansen and Veum (1990); G = Grobe *et al.* (1990); S = Shackleton, unpublished; C & F = Charles and Fairbanks (1990); K & B = Keigwin and Boyle (1989); E. V. = E. Vogelsang thesis (1990); T. Veum: T. Veum thesis (1990).*

Données utilisées pour la calibration de la composition isotopique de l'oxygène de *Neogloboquadrina pachyderma* (sénestre).

Les latitudes et longitudes sont exprimées en degrés et minutes ; les valeurs positives indiquent respectivement le Nord et l'Est, les valeurs négatives le Sud et l'Ouest. La température et la salinité des eaux de surface sont extraites de l'atlas de Levitus (1982). La composition isotopique de l'oxygène ( $\delta^{18}\text{O}$ ) des eaux superficielles a été calculée à partir des droites de régression des figures 2A et 2B.

Sources des données : D = Durazzi (1981) ; M & F = Mix et Fairbanks (1985) ; KDS = Kellogg *et al.* (1978) ; Gif = analyses faites à Gif pour ce travail ; J & V = Jansen et Veum (1990) ; G = Grobe *et al.* (1990) ; S = Shackleton, données non publiées : C & F = Charles et Fairbanks (1990) ; K & B = Keigwin et Boyle (1989) ; E. V. = thèse d'E. Vogelsang (1990) ; T. Veum = thèse de T. Veum (1990).

Core	Latitude	Longitude	$\delta^{18}\text{O}$ left coiling <i>N. pachyderma</i>	Summer sea surface salinity	Calculated sea surface $\delta^{18}\text{O}$	Summer sea surface temperature	Isotopic temperature	Data source
<b>North Atlantic</b>								
FRAM-1/4	84.30	- 8.59	2.07	31.1	- 1.91	- 1.3	0.10	MZT
FRAM-1/7	83.53	- 6.57	2.03	31	- 1.96	- 1.1	0.05	MZT
V 27.60	72.11	8.35	2.78	35.2	0.38	8.3	5.92	Gif
K-11	71.47	1.36	3.02	35.2	0.38	6.5	5.01	Gif
23 043-3	70.16	- 3.21	2.75	35.1	0.33	7.4	5.83	E.V.
71-17	70.01	- 13.01	3.68	34.2	- 0.18	4.2	0.53	E.V.
71-15	70.00	- 17.26	3.72	33.5	- 0.57	3.1	- 0.98	E.V.
V 30-164	69.50	8.58	2.37	35.2	0.38	8.7	7.52	S
23 061-3	69.30	- 2.02	2.64	35.2	0.38	8.3	6.46	E.V.
71-19	69.29	- 9.31	3.38	34.8	0.16	6	2.83	E. V.
V 28-38	69.23	- 4.24	2.8	35.1	0.33	7.6	5.63	Gif
23 243-2	69.23	- 6.33	3.08	34.9	0.21	7	4.15	E. V.
23 246-2	69.23	- 12.55	3.82	34.5	- 0.01	5.3	0.63	E. V.
23 062-3	68.43	0.11	2.6	35.2	0.38	9.2	6.62	E. V.
23 041-1	68.42	- 0.14	2.55	35.2	0.38	9.2	6.81	E. V.
23 057-1	68.40	3.30	2.65	35.3	0.44	9.8	6.64	E. V.
23 064-2	68.40	0.20	2.51	35.2	0.38	9.2	6.97	E. V.
23 056-2	68.30	3.50	2.78	35.3	0.44	9.8	6.14	E. V.
23 055-2	68.25	4.02	2.43	35.3	0.44	10	7.50	E. V.
V 28-56	68.02	- 6.07	2.86	35	0.27	7.5	5.19	KDS
23 068-2	67.50	1.30	2.45	35.2	0.38	9.8	7.20	E. V.
23 038-3	67.44	5.55	2.36	35.1	0.33	10.5	7.34	E. V.
23 069-2	67.40	1.36	2.46	35.2	0.38	9.8	7.17	E. V.
23 039-3	67.39	5.48	2.44	35.1	0.33	10.5	7.03	E. V.
23 070-2	67.21	2.10	2.3	35.3	0.44	10	8.01	E. V.
23 071-2	67.05	2.55	2.4	35.3	0.44	10	7.62	E. V.
23 040-3	67.00	7.47	2.42	34.8	0.16	10.8	6.45	E. V.
23 072-2	67.00	3.25	2.36	35.2	0.38	10.2	7.56	E. V.
23 074-3	66.41	4.55	2.45	35	0.27	10.7	6.77	E. V.
V 27-86	66.36	1.07	2.63	35.2	0.38	9.8	6.50	Gif
23 037-2	65.31	- 0.07	2.51	35.2	0.38	10.2	6.97	E. V.
V 28-14	64.47	- 29.34	2.15	34.6	0.05	7.9	7.07	Gif
HM 52-43	63.31	0.44	2.01	35.2	0.38	10.9	8.95	T. Veum
HU 75-41	62.39	- 53.53	2.73	33.5	- 0.57	5.5	2.55	Gif
HU 75-42	62.39	- 53.54	2.66	33.5	- 0.57	5.5	2.81	Gif
CH 73-110	59.30	- 8.56	2.67	35.3	0.44	11.9	6.56	Gif
V 30-126	58.34	- 35.30	2.35	35.1	0.33	10.2	7.38	D
V 23-23	56.05	- 44.33	2.35	34.7	0.10	9.7	6.51	M & F
CH 73-139c	54.38	- 16.21	2.47	35.4	0.49	14	7.56	Gif
V 23-81	54.15	- 16.50	1.1	35.4	0.49	14	13.14	J & V
V23-22	54.12	- 46.00	1.76	34.5	- 0.01	10.3	8.38	D
<b>Southern Ocean</b>								
RC 15-94	- 42.54	- 20.51	0.9	34.3	- 0.07	10.9	11.61	C & F
V 22-108	- 43.11	- 3.15	1	34.24	- 0.10	9.77	11.07	C & F
MD 87-716	- 43.46	- 15.32	2.97	34.2	- 0.13	9.9	3.29	Gif
MD 73-025	- 43.49	51.19	2.16	33.7	- 0.40	9.5	5.31	Gif
MD 84-527	- 43.49	51.19	2.06	33.7	- 0.40	9.5	5.69	Gif
MD 73-026	- 44.59	53.17	2	33.7	- 0.40	9.45	5.92	Gif

Table 2 (cont.)

Core	Latitude	Longitude	$\delta^{18}\text{O}$ left coiling <i>N. pachyderma</i>	Summer sea surface salinity	Calculated sea surface $\delta^{18}\text{O}$	Summer sea surface temperature	Isotopic temperature	Data source
MD 88-770	- 46.01	96.28	1.94	34	- 0.24	8.1	6.78	Gif
MD 88-769	- 46.04	90.07	1.44	34.2	- 0.13	9.7	9.19	Gif
RC 13-254	- 48.34	5.07	2.5	33.84	- 0.32	4.58	4.31	C & F
MD 80-304	- 51.04	67.44	2.83	33.9	- 0.29	4.6	3.20	Gif
MD80-KK63	- 51.56	42.53	3.3	33.8	- 0.35	2.54	1.28	Gif
RC 13-271 -	51.59	4.31	2.82	33.86	- 0.31	2.5	3.15	C & F
CHN115-36PG	- 52.20	6.30	3.26	33.9	- 0.29	2.43	1.63	K & B
RC 13-269	- 52.37	0.07	2.8	33.84	- 0.32	1.77	3.19	C & F
MD 88-773	- 52.54	109.52	2.93	33.9	- 0.29	3	2.83	Gif
MD 84-560	- 53.07	72.10	2.43	33.9	- 0.29	2.49	4.70	Gif
CHN115-26PG	- 53.36	- 0.06	3.05	33.84	- 0.32	1.77	2.27	K & B
MD 82-424	- 54.06	- 0.22	3.48	33.84	- 0.32	1.3	0.72	Gif
MD 88-784	- 54.12	144.48	2.97	33.8	- 0.35	5.1	2.48	Gif
CHN115-27PG	- 54.42	- 2.05	3.28	33.9	- 0.29	0.98	1.55	K & B
AII-107/22-	- 54.48	- 3.20	3.38	33.9	- 0.29	1	1.19	K & B
MD 84-552	- 54.55	75.50	3.15	33.9	- 0.29	1.93	2.02	Gif
MD 84-551	- 55.00	73.17	3.15	33.9	- 0.29	2.04	2.02	Gif
KR MD 88-13	- 57.57	144.35	3.3	33.8	- 0.35	3.96	1.28	Gif
M269-965	- 60.54	- 57.06	3.2	34	- 0.24	0.82	2.04	K & B
PS 1 387	- 68.44	- 5.52	3.59	33.6	- 0.45	- 0.56	- 0.14	G
PS 1 431	- 69.49	- 6.35	3.46	33.6	- 0.45	- 0.6	0.32	G
PS 1 394	- 70.06	- 6.51	3.4	33.6	- 0.45	- 0.6	0.54	G

*G. bulloides*, this regression line differs by less than 0.7°C from the simple relationship :  $T_{\text{isotope}} = \text{summer SST minus } 1^{\circ}\text{C}$  (Fig. 3B). Whereas the estimate of the isotopic temperature provided by the regression line has a standard deviation of 1.17°C, that obtained with the simple linear relationship has a standard deviation of 1.21°C. We shall therefore use the relationship  $T_{\text{isotope}} = \text{summer SST minus } 1^{\circ}\text{C}$  as a calibration for *G. bulloides*.

We calibrated *N. pachyderma* (left coiling) by analyzing 69 cores distributed throughout the North Atlantic Ocean and the Southern Ocean and raised from locations where summer SST ranges from - 1.3°C to 14°C (Tab. 2). We did not try to analyze separately the different ecophenotypes of this species (Kennett and Srinivasan, 1980), because, although they sometimes display different isotopic compositions (Williams *et al.*, 1981), no clear trend can be depicted at the level of a large basin like the Norwegian Sea

(Johannessen, 1987). Separate dw/salinity relationships derived from the GEOSECS measurements (Fig. 2) were used for each basin and the isotopic temperatures calculated in the same way as in Table 1. Comparison of the Levitus (1982) summer SST with that derived from the  $\delta^{18}\text{O}$  value of *N. pachyderma* (Fig. 4) shows trends similar to those observed for *G. bulloides*. In the temperature range 3 to 10°C, the isotopic temperature given by *N.*

Figure 4

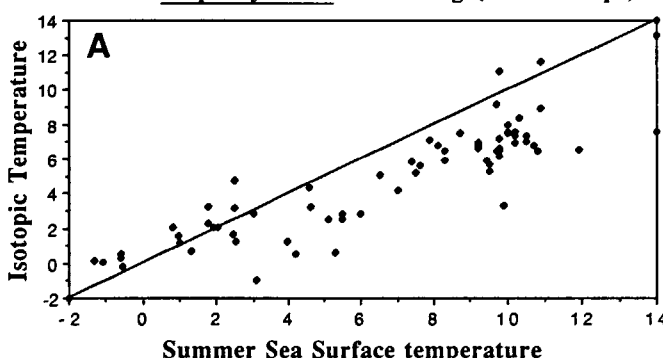
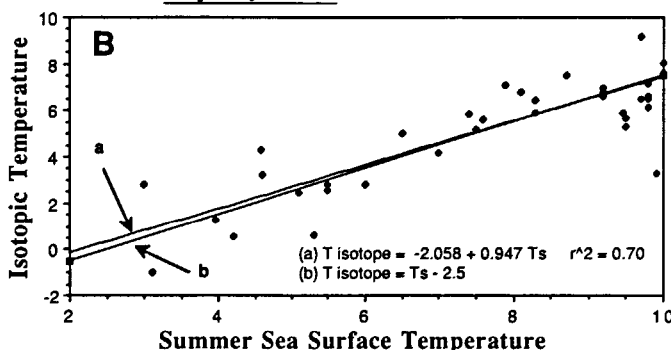
A: Plot of the isotopic temperature calculated from *N. pachyderma* (left coiling)  $\delta^{18}\text{O}$  values against summer sea surface temperature for 69 core tops from the North Atlantic and Southern oceans.

B: Comparison of the regression line (a) calculated for samples for which the summer SST is in the range 3-10°C, with the linear relationship (b):  $T_{\text{isotope}} = \text{summer SST} - 2.5^{\circ}\text{C}$ .

A : Variations, en fonction de la température d'été des eaux superficielles, de la température isotopique calculée à partir de la composition isotopique ( $\delta^{18}\text{O}$ ) de *N. pachyderma* sénestre.

69 sommets de carottes provenant de l'Océan Atlantique Nord, de la mer de Norvège et de l'Océan Austral ont été utilisés.

B : Comparaison de la droite de régression (a), calculée pour les échantillons provenant de carottes pour lesquelles la température d'été des eaux de surface est comprise entre 3 et 10°C, avec la droite (b) d'équation :  $T_{\text{isotope}} = \text{température d'été des eaux superficielles} - 2.5^{\circ}\text{C}$ .

Modern *N. pachyderma* left coiling (69 core tops)Modern *N. pachyderma* (3°C < Summer SST < 10°C)

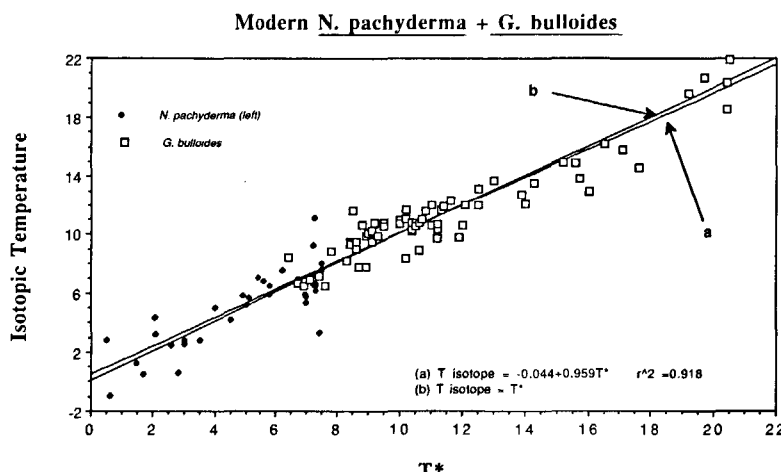


Figure 5

Plot of the isotopic temperature calculated from  $\delta^{18}\text{O}$  values of *G. bulloides* and *N. pachyderma* (left coiling) which grew in their optimum temperature range against the effective temperature of calcification  $T^*$ .

Variations, en fonction de la température de calcification  $T^*$ , de la température isotopique calculée à partir des valeurs de  $\delta^{18}\text{O}$  de *G. bulloides* et de *N. pachyderma* (sénestre) ayant vécu dans leur domaine optimal de température.

*pachyderma* covaries with the summer SST, whereas in warmer waters, isotopic temperature values exhibit a noticeable scatter (Fig. 4A). Within the temperature range -1.5°C to 3°C, the isotopic temperatures given by *N. pachyderma* are in the range 0-3°C, and are often warmer than the atlas mean summer values. This is true even when a permanent ice cover is generally present at the surface. This indicates that, in very cold water, *N. pachyderma* develops only when it can find a water mass whose temperature is close to 0-1°C.

*N. pachyderma* is known to be a cold-water species (Bé, 1960; Bé and Tolderlund, 1971). We interpret the trend depicted in Figure 4A as an indication that this foraminifer lives only within a well-defined temperature range. It develops only during the warmest month in the coldest waters, and during the summer and spring season in subpolar waters, when water stratification and relatively low temperatures allow the simultaneous development of phytoplankton and of *N. pachyderma*. This interpretation is in agreement with sediment trap experiments which show the occurrence of *N. pachyderma* (left coiling) in January close to Antarctica and mainly during spring in the Northeast Pacific (Wefer *et al.*, 1988; Reynolds-Sautter and Thunell, 1989). A statistical analysis performed on core tops raised from locations where the summer SST is

in the range +3/+10°C shows that the isotopic temperature given by *N. pachyderma* is linearly correlated to the summer SST ( $r^2 = 0.70$ ) and that the best fit line has a slope (0.947 with  $\sigma = 0.04$ ) which is not significantly different from 1 at the 2  $\sigma$  level. Over the whole "optimal temperature range" of *N. pachyderma* (left coiling), this regression line differs by less than 0.4°C from the value calculated by subtracting 2.5°C from the summer SST (Fig. 4B). Whereas the estimate of the isotopic temperature provided by the regression line has a standard deviation of 1.50°C, that obtained by subtracting 2.5°C from the summer SST has a standard deviation of 1.51°C. We shall henceforth consider that the optimal temperature range for *N. pachyderma* is +3°C < summer SST < +10°C and use the simple linear relationship  $T_{\text{isotope}} = \text{summer SST} - 2.5^\circ\text{C}$  as a calibration for *N. pachyderma* (left coiling).

We therefore define a parameter, which we call  $T^*$ , and which represents a statistical estimate of the mean calcification temperature for each species :  $T^* = \text{summer SST} - 1^\circ\text{C}$  for *G. bulloides* and  $T^* = \text{summer SST} - 2.5^\circ\text{C}$  for *N. pachyderma*. Taking all the *N. pachyderma*  $\delta^{18}\text{O}$  values from sites where the summer SST is higher than 3°C and lower than 10°C and all the *G. bulloides*  $\delta^{18}\text{O}$  values from sites where the summer SST is higher than 7°C and lower than 22°C, we find that the isotopic temperatures calcula-

Table 3

#### Summary of the data used to reconstruct the North Atlantic sea surface salinity during the last ice age.

Ice age summer SST was estimated from the CLIMAP (1981) reconstruction when no faunal temperature estimates were available. Ice age sea surface delta O-18 was calculated assuming isotopic equilibrium with  $T^*$  defined in the text. Modern sea surface delta O-18 was calculated from the Levitus (1982) salinity data and the regression line of Figure 2A. The ice age sea surface delta O-18 anomaly was calculated as difference between ice age and modern values minus the global ice volume effect.

Data Source : 1 = Markussen *et al.*, 1985; 2 = Labeyrie *et al.*, 1987; 3 = Duplessy *et al.*, 1975; 4 = Kellogg *et al.*, 1978; 5 = Labeyrie and Duplessy, 1985; 6 = Grousset and Duplessy, 1983; 7 = Keigwin and Boyle, 1989; 8 = Sejrup *et al.*, 1984; 9 = analyses made at Gif for this work; 10 = Fillon and Duplessy, 1980; 11 = Hillaire Marcel and de Vernal, 1989; 12 = Aksu *et al.*, 1989; 13 = Scott *et al.*, 1989; 14 Mix and Fairbanks, 1985; 15 = Jansen and Veum, 1990; 16 = Zahn, 1986; 17 = Shackleton, unpublished.

Données utilisées pour la reconstruction de la salinité des eaux superficielles de l'Océan Atlantique Nord au cours du dernier maximum glaciaire. Les latitudes et longitudes sont exprimées en degrés et minutes ; les valeurs positives indiquent respectivement le Nord et l'Est, les valeurs négatives le Sud et l'Ouest. La salinité actuelle des eaux de surface est extraite de l'atlas de Levitus (1982). La composition isotopique de l'oxygène ( $\delta^{18}\text{O}$ ) des eaux superficielles a été calculée à partir de la droite de régression de la figure 2A. L'anomalie de  $\delta^{18}\text{O}$  des eaux superficielles a été calculée comme différence entre la valeur glaciaire et la valeur actuelle et corrigée de l'effet des variations du volume des glaces continentales.

Sources des données : 1 = Markussen *et al.* (1985); 2 = Labeyrie *et al.* (1987); 3 = Duplessy *et al.* (1975); 4 = Kellogg *et al.* (1978); 5 = Labeyrie et Duplessy (1985); 6 = Grousset et Duplessy (1983); 7 = Keigwin et Boyle (1989); 8 = Sejrup *et al.* (1984); 9 = analyses faites à Gif pour ce travail : 10 = Fillon et Duplessy (1980); 11 = Hillaire-Marcel et de Vernal (1989); 12 = Aksu *et al.* (1989); 13 = Scott *et al.* (1989); 14 = Mix et Fairbanks (1985); 15 = Jansen et Veum (1990); 16 = Zahn (1986); 17 = Shackleton, données non publiées.

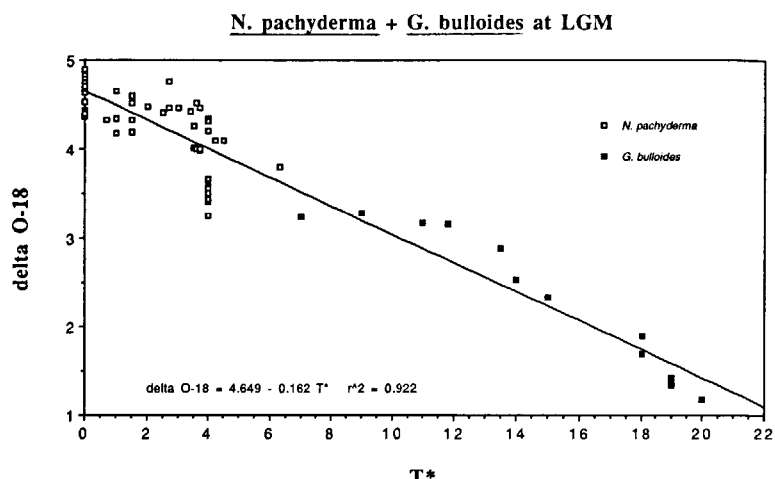
## SALINITY OF THE GLACIAL NORTH ATLANTIC OCEAN

Core	Latitude	Longitude	Foram.	Ice age								Data source
				Summer	Foram.	SST	$\delta^{18}\text{O}$	Sea surface	Modern	Modern	Sea surface	$\delta^{18}\text{O}$
FRAM-1/4	84.30	- 8.59	pachy	0.0	4.7	0.69	31.10	- 1.91	1.40	34.94	34.94	1
FRAM-1/7	83.53	- 6.57	pachy	0.0	4.69	0.68	31.10	- 1.91	1.39	34.92	34.92	1
V27-60	72.1	8.35	pachy	0.0	4.72	0.71	35.20	0.44	- 0.93	34.38	34.38	2
K11	71.47	1.36	pachy	0.0	4.71	0.70	35.20	0.38	- 0.88	34.48	34.48	3
V 30-164	69.50	8.58	pachy	0.0	4.83	0.82	35.20	0.38	- 0.76	34.72	34.72	17
V28-38	69.23	- 4.24	pachy	0.0	4.78	0.77	35.10	0.33	- 0.76	34.62	34.62	2
V28-56	68.02	- 6.07	pachy	0.0	4.78	0.77	35.00	0.27	- 0.70	34.64	34.64	4
V27-86	66.36	1.07	pachy	0.0	4.73	0.72	35.20	0.38	- 0.86	34.52	34.52	5
CH77-07	66.36	- 10.31	pachy	0.0	4.72	0.71	34.85	0.19	- 0.68	34.53	34.53	6
V29-206	64.54	- 29.17	pachy	0.0	4.37	0.36	34.70	0.10	- 0.94	33.86	33.86	7
V28-14	64.47	- 29.34	pachy	0.0	4.64	0.63	34.60	0.05	- 0.62	34.40	34.40	4
31-36	64.15	0.31	pachy	0.0	4.88	0.87	35.10	0.33	- 0.66	34.82	34.82	8
31-33	63.38	1.46	pachy	0.0	4.44	0.43	35.00	0.27	- 1.04	33.96	33.96	8
HU 75-58	62.46	- 59.22	pachy	0.0	4.53	0.52	33.30	- 0.68	0.00	34.34	34.34	9
HU 75-41	62.39	- 53.52	pachy	0.0	4.89	0.88	33.50	- 0.57	0.25	35.04	35.04	10
HU 75-42	62.39	- 53.54	pachy	0.0	4.75	0.74	33.50	- 0.57	0.11	34.76	34.76	10
NO 77-14	62.27	- 20.25	pachy	2.0	4.65	0.93	35.20	0.38	- 0.65	34.92	34.92	9
V23-42	62.11	- 27.56	pachy	2.5	4.52	0.93	35.33	0.45	- 0.72	34.93	34.93	7
CH 73-110	59.30	- 8.56	pachy	0.0	4.4	0.39	35.30	0.38	- 1.19	33.96	33.96	9
HU 75-37	59.09	- 48.23	pachy	0.0	4.4	0.39	34.14	- 0.21	- 0.60	33.98	33.98	11
KN714-15	58.46	- 25.57	pachy	5.0	4.41	1.10	35.22	0.39	- 0.49	35.27	35.27	7
ODP 646	58.13	- 48.56	pachy	0.0	4.42	0.41	34.55	0.02	- 0.81	33.97	33.97	12
HU84-030-004	58.13	- 48.56	pachy	0.0	4.7	0.69	34.55	0.02	- 0.53	34.53	34.53	13
CH 73-108	58.05	- 10.43	pachy	2.0	4.18	0.46	35.30	0.44	- 1.18	33.96	33.96	9
V30-108	56.06	- 38.44	pachy	4.5	4.48	1.03	34.72	0.11	- 0.28	35.20	35.20	7
V23-23	56.05	- 44.33	pachy	3.5	4.34	0.62	34.70	0.10	- 0.68	34.36	34.36	14
CH73-136	55.34	- 14.28	pachy	6.0	4.26	1.22	35.40	0.49	- 0.47	35.49	35.49	9
V27-114	55.03	- 33.04	pachy	5.5	4.46	1.29	34.75	0.13	- 0.04	35.69	35.69	7
RC9-225	54.59	- 15.24	pachy	6.2	3.99	1.00	35.38	0.48	- 0.68	35.06	35.06	7
CH 73-139	54.38	- 16.21	pachy	6.0	4.02	0.98	35.40	0.49	- 0.71	35.01	35.01	9
NO 79-06	54.31	- 36.53	pachy	5.2	4.76	1.50	34.66	0.08	0.22	36.14	36.14	9
V23-81	54.15	- 16.50	pachy	6.1	4	0.99	35.39	0.49	- 0.70	35.01	35.01	15
V27-20	54.00	- 46.12	pachy	3.2	4.33	0.52	34.40	- 0.06	- 0.62	34.19	34.19	7
ODP 647	53.20	- 45.16	pachy	4.0	4.19	0.60	34.28	- 0.13	- 0.47	34.38	34.38	12
HU84-030-001	53.20	- 45.16	pachy	4.0	4.6	1.01	34.28	- 0.13	- 0.06	35.20	35.20	13
HU84-030-003	53.20	- 45.16	pachy	4.0	4.32	0.73	34.28	- 0.13	- 0.34	34.64	34.64	11
CH 73-141	52.52	- 16.31	pachy	6.2	4	1.01	35.40	0.49	- 0.68	35.08	35.08	9
V27-116	52.50	- 30.20	pachy	6.1	4.52	1.51	34.92	0.23	0.08	36.10	36.10	7
V23-82	52.35	- 21.56	pachy	6.5	4.34	1.43	35.31	0.44	- 0.21	35.93	35.93	7
V27-19	52.06	- 38.48	pachy	5.2	4.46	1.20	34.70	0.10	- 0.10	35.54	35.54	7
KN708-6	51.34	- 29.34	pachy	6.2	4.46	1.47	35.01	0.28	- 0.01	36.03	36.03	7
V27-17	50.05	- 37.18	pachy	5.9	4.42	1.35	35.00	0.27	- 0.12	35.80	35.80	7
KN 708-1	50.00	- 23.45	pachy	6.5	4.21	1.30	35.46	0.53	- 0.43	35.64	35.64	7
V23-83	49.52	- 24.15	pachy	6.5	4.31	1.40	35.46	0.53	- 0.33	35.84	35.84	7
V29-183K	49.08	- 25.30	pachy	6.7	4.1	1.25	35.50	0.55	- 0.50	35.53	35.53	7
CH 72-101	47.28	- 8.34	pachy	6.5	3.51	0.60	35.56	0.58	- 1.18	34.24	34.24	9
NO 79-25	46.59	- 27.17	pachy	7.0	4.1	1.33	35.70	0.66	- 0.53	35.67	35.67	9
CH 72-104	46.54	- 8.05	pachy	6.5	3.25	0.34	35.52	0.56	- 1.42	33.72	33.72	9
NO 79-29	46.18	- 15.04	bullo	8.0	3.23	1.11	35.75	0.69	- 0.78	35.22	35.22	9
CH 69-12	46.01	- 4.41	pachy	6.5	3.65	0.74	35.29	0.43	- 0.89	34.55	34.55	9
CH 67-19	45.45	- 3.57	pachy	6.5	3.57	0.66	35.13	0.34	- 0.88	34.41	34.41	9
CH 69-32	45.24	- 5.10	pachy	6.5	3.56	0.65	35.30	0.44	- 0.99	34.36	34.36	9
V29-180	45.18	- 23.52	pachy	8.8	3.8	1.50	35.77	0.70	- 0.40	36.00	36.00	7
SU 81-47	44.53	- 3.18	pachy	6.5	3.44	0.53	34.93	0.23	- 0.90	34.17	34.17	9
CH 66-03	44.05	- 2.11	pachy	6.5	3.41	0.50	34.85	0.19	- 0.89	34.11	34.11	9
CH69-69	43.51	- 4.30	pachy	6.5	3.66	0.75	35.17	0.36	- 0.81	34.59	34.59	9
NO 79-17	43.00	- 27.10	bullo	12.8	3.16	2.23	35.91	0.78	0.25	37.45	37.45	9
SU 81-32	42.06	- 9.47	bullo	10.0	3.27	1.66	35.80	0.72	- 0.26	36.30	36.30	9
S 8-79-04	42.00	- 22.00	bullo	14.5	2.87	2.35	35.95	0.80	0.35	37.68	37.68	9
CH 69-09	41.45	- 47.21	bullo	12.0	3.17	2.05	34.54	0.01	0.84	37.25	37.25	9
SU81-18	37.46	- 10.11	bullo	16.0	2.32	2.15	36.10	0.88	0.07	37.27	37.27	9
SU81-14	36.46	- 9.51	bullo	15.0	2.52	2.12	36.30	1.00	- 0.08	37.17	37.17	9
M 15672	34.52	- 8.08	bullo	16.0	2.32	2.15	36.48	1.10	- 0.15	37.21	37.21	16
M 15637	27.00	- 18.59	bullo	19.0	1.89	2.41	36.85	1.30	- 0.09	37.70	37.70	16
M 12309	26.50	- 15.07	bullo	19.0	1.69	2.21	36.60	1.16	- 0.15	37.33	37.33	16
M 13289	18.04	- 18.01	bullo	20.0	1.42	2.16	35.80	0.72	0.24	37.32	37.32	16
M 12347	15.50	- 17.52	bullo	20.0	1.34	2.08	35.44	0.52	0.36	37.20	37.20	16
M 12345	15.29	- 17.22	bullo	20.0	1.35	2.09	35.02	0.28	0.61	37.28	37.28	16
M 13239	13.53	- 18.19	bullo	21.0	1.18	2.15	35.03	0.29	0.66	37.37	37.37	16

**Figure 6**

**A: Plot of the  $\delta^{18}\text{O}$  value of *G. bulloides* and *N. pachyderma* (left coiling) which grew in their optimum temperature ranges during the last glacial maximum against the effective temperature of calcification  $T^*$  calculated from summer sea surface temperature estimated by CLIMAP (1981).**

Variations, en fonction de la température de calcification  $T^*$  calculée à partir des données CLIMAP (1981), de la composition isotopique  $\delta^{18}\text{O}$  de *G. bulloides* et de *N. pachyderma* (sénestre) ayant vécu dans leur domaine optimal de température au cours du dernier maximum glaciaire.



ted from the  $\delta^{18}\text{O}$  values of these species are not significantly different from the temperature  $T^*$  (Fig. 5). They are highly correlated ( $r^2 = 0.918$ ) and the slope of the regression line (0.959 with  $\sigma = 0.04$ ) is not significantly different from 1 at the  $2\sigma$  level. We shall assume in the following section that this statistical relationship is also valid under glacial climatic conditions. These data, which provide an empirical calibration of the  $\delta^{18}\text{O}$  variations of both foraminiferal species against summer temperature, strongly suggest an important limitation:  $\delta^{18}\text{O}$  analysis may be used to reconstruct summer surface salinity, but will not allow direct reconstruction of the salinity field during winter conditions. This is an important season for the oceanic circulation since sinking of surface waters occurs during the coldest months of the year.

## GLACIAL PATTERN FOR *G. BULLOIDES* AND *N. PACHYDERMA*

We consider (Tab. 3) only cores located in areas where the ice age summer SST reconstructed by CLIMAP (1981)

was lower than 22°C and in which *G. bulloides* or *N. pachyderma* have lived in the respective optimum temperature ranges defined above. Our coverage comprises a large fraction of the glacial North Atlantic, from the northern subtropical zone to areas covered with sea ice. We discarded cores located in areas of strong upwelling, because we have no calibration for these particular situations. Where the CLIMAP reconstruction indicated summer SST lower than 1°C or the presence of permanent sea ice, we assumed that the temperature recorded by *N. pachyderma* was  $T^* = 0^\circ\text{C}$ , which agrees with the calibration performed on modern samples. For each core, the LGM  $\delta^{18}\text{O}$  value was estimated from the isotopic record by taking either the maximum  $\delta^{18}\text{O}$  value, in cores where the sedimentation rate was low, or the mean  $\delta^{18}\text{O}$  value of the isotope stage 2 maximum. A linear trend between the foraminiferal  $\delta^{18}\text{O}$  values and the  $T^*$  value calculated from the CLIMAP summer SST is clearly present in the data (Fig. 6). Two major features appear : first, the linear regression line has a slope of 0.162 and does not parallel the predicted isotopic equilibrium line (mean slope 0.25). This agrees with previous observations made on *N. pachyderma* by Keigwin and Boyle (1989) and indicates that the surface salinity varied along with temperature; second, this

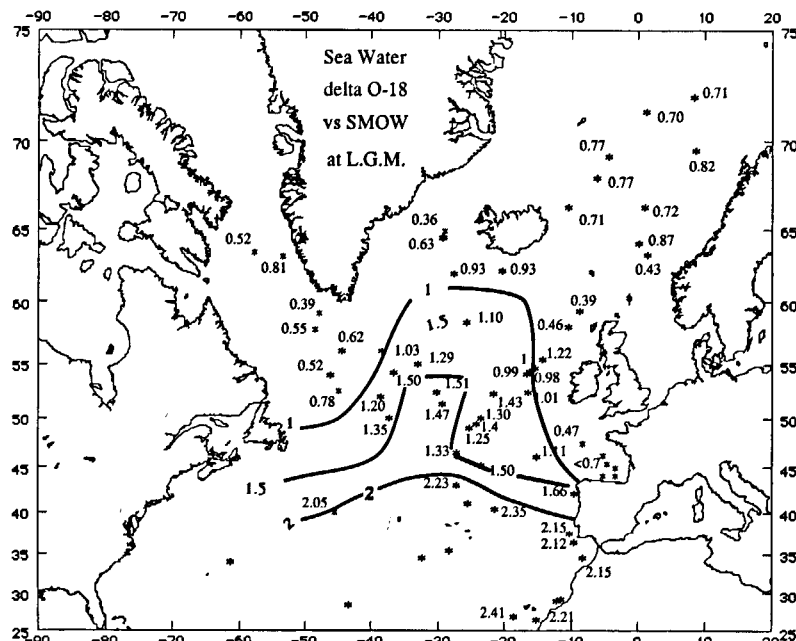


**Figure 7**

*Reconstruction of the summer sea surface water  $\delta^{18}\text{O}$  (vs SMOW) for the North Atlantic Ocean during the last glacial maximum.*

Reconstitution de la composition isotopique de l'oxygène ( $\delta^{18}\text{O}$  vs SMOW) de l'eau superficielle de l'Océan Atlantique Nord au cours du dernier maximum glaciaire.

regression line has a high correlation coefficient ( $r^2 = 0.922$ ), indicating that the relationship linking the summer surface-seawater  $\delta^{18}\text{O}$  value to summer SST was approximately linear, as observed in the modern ocean.

### GLACIAL SEA SURFACE WATER $\delta^{18}\text{O}$ PATTERNS

In Table 3, we calculate the summer surface-water  $\delta^{18}\text{O}$  value, assuming that the foraminifera grew their shells in isotopic equilibrium with  $T^*$ . We assume that  $T^* = +0^\circ\text{C}$  for *N. pachyderma* samples when the summer SST estimate is lower than  $1^\circ\text{C}$ .

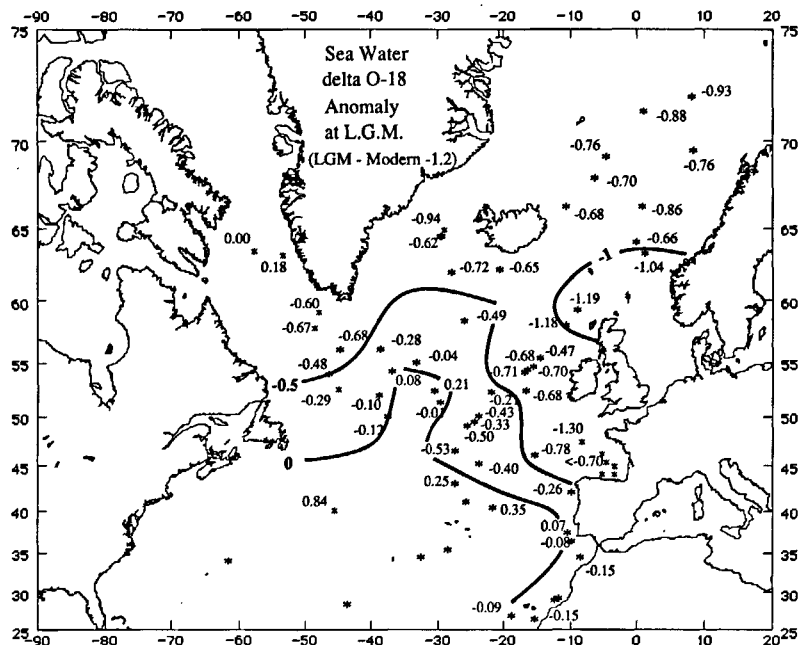
Recent estimates for the  $\Delta$  value range from 1.1 to 1.3 ‰ (Labeyrie *et al.*, 1987; Shackleton, 1987; Fairbanks, 1989). We therefore adopted the mean value of 1.2 ‰ to compute the anomaly map (Fig. 8).

Negative anomalies are generally found north of the polar front. This is particularly marked in the Bay of Biscay as a consequence of the outflow of European rivers, which carried meltwater from snow and from the southern margin of the ice sheets. This water was depleted in  $^{18}\text{O}$  with respect to the mean ocean water. Negative anomalies are also seen in the Norwegian-Greenland seas as a consequence of the disappearance of the North Atlantic drift during glacial conditions (Kellogg, 1976; Ruddiman and McIntyre, 1973; Alvinerie *et al.*, 1978). The most negative values are found

Figure 8

Map of the summer sea-surface  $\delta^{18}\text{O}$  anomaly ( $(\delta^{18}\text{O}_{\text{LGM}} - \delta^{18}\text{O}_{\text{modern}}) - 1.2\text{ ‰}$ ) for the North Atlantic Ocean during the last glacial maximum.

Carte de l'anomalie de  $\delta^{18}\text{O}$  ( $\delta^{18}\text{O}_{\text{LGM}} - \delta^{18}\text{O}_{\text{moderne}} - 1,2\text{ ‰}$ ) des eaux superficielles de l'Océan Atlantique Nord au cours du dernier maximum glaciaire.



The  $\delta^{18}\text{O}$  values (vs. SMOW) are plotted in Figure 7. Clearly these were high in northern subtropical waters and exhibited a decreasing trend toward high latitudes. A marked gradient coincided with the thermal polar front, except in the middle Atlantic between 30 and  $40^\circ\text{W}$ . Surface waters in the Norwegian-Greenland seas were under permanent sea-ice and exhibited rather constant low  $\delta^{18}\text{O}$  values, close to  $+0.75\text{ ‰}$ . The lowest values are found close to Greenland and the European continent, near the edge of the permanent sea-ice, and also in the Bay of Biscay, although this area was not ice covered even during winter (CLIMAP, 1981).

In order to compare with the modern pattern, we calculated the  $\delta^{18}\text{O}$  anomaly as the difference between the LGM  $\delta^{18}\text{O}$  values minus the modern  $\delta^{18}\text{O}$  value and corrected this difference from the mean oceanic  $\delta^{18}\text{O}$  change ( $\Delta$ ) due to the growth of continental ice sheets :

$$\delta^{18}\text{O} (\text{anomaly}) = \delta^{18}\text{O} (\text{LGM}) - \delta^{18}\text{O} (\text{modern}) - \Delta (\text{ice volume}).$$

in the area of the North Atlantic which was only seasonally covered by sea ice. This pattern suggests that icebergs originating from continental ice sheets, composed of ice impoverished in  $^{18}\text{O}$ , also melted in this area. Both the negative  $\delta^{18}\text{O}$  anomalies off west Ireland and Faeroe and that in the Bay of Biscay imply a southward eastern boundary current, carrying icebergs and meltwater in a direction opposite to that of today.

The presence of the Labrador current along the eastern coast of North America is marked by  $\delta^{18}\text{O}$  values noticeably lower than those found in the central Atlantic at about  $50-55^\circ\text{N}$ . In contrast, positive anomalies are found north of the polar front, from  $45$  to  $55^\circ\text{N}$  and from  $30$  to  $40^\circ\text{W}$ . The presence of a surface water mass isotopically comparatively heavier than the modern one indicates the occurrence of a significant flux of salt, north of the polar front.

In order to estimate the salinity of the surface waters, we need to know the slope of the salinity/ $\delta^{18}\text{O}$  relationship for the glacial ocean. At present we have no way to estimate

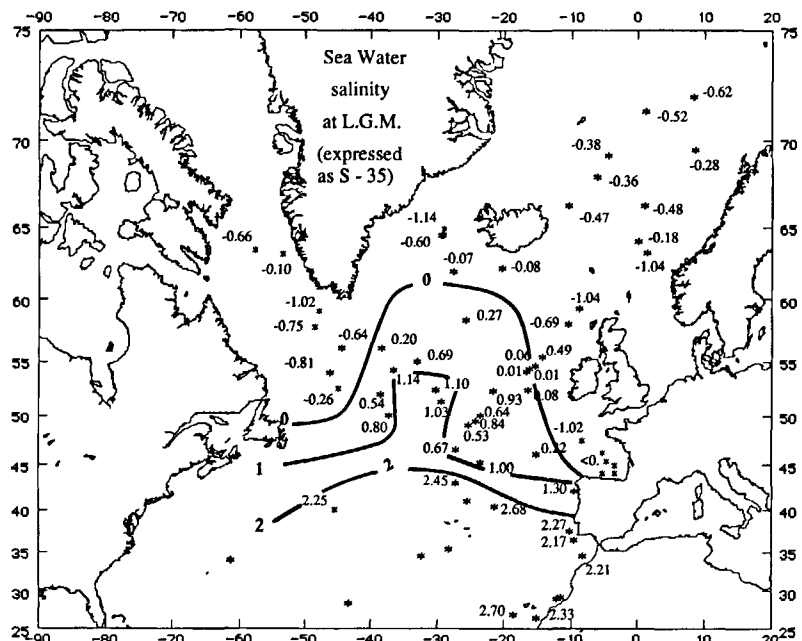


Figure 9

Map of the summer sea-surface salinity reconstruction for the North Atlantic Ocean during the last glacial maximum.

Reconstitution de la salinité des eaux superficielles de l'Océan Atlantique Nord au cours du dernier maximum glaciaire.

this slope without relying on atmospheric general circulation models which also simulate the transport of water isotopic molecules (Joussaume, 1989). As these simulations are not precise, we adopt here the mean value of the slope of the salinity/ $\delta^{18}\text{O}$  relationship for the modern ocean and assume that the salinity increased by 2 when the sea water  $\delta^{18}\text{O}$  value increased by 1 (Craig and Gordon, 1965). However, in order to minimize the effect of the uncertainty in this slope, we do not calculate the glacial salinity directly from the glacial  $\delta^{18}\text{O}$  value. We first correct the modern salinity value for the global salinity increase due to the formation of continental ice sheets. We then apply the salinity  $\delta^{18}\text{O}$  relationship only to the  $\delta^{18}\text{O}$  anomaly reported in Table 3. The present mean ocean salinity is 34.7. As the present mean ocean water depth is 3 900 m and as the sea level was lower than today by 120 m during glacial conditions (Fairbanks, 1989), the mean glacial salinity was higher than the modern one by  $34.7 \times 120/3 780 = 1.04$ . We therefore calculated the summer surface water salinity for the glacial North Atlantic Ocean as:

$$S_{\text{glacial}} = S_{\text{modern}} + 1.04 + (2 \times \delta^{18}\text{O} \text{ anomaly}).$$

As expected, the reconstruction obtained in Figure 9 exhibits trends similar to those depicted on the map Figure 7, since the salinity estimates are linearly linked with the sea surface  $\delta^{18}\text{O}$  values.

## DISCUSSION AND CONCLUSION

Like all the paleoclimatic reconstructions based on the oxygen isotopic composition of individual foraminiferal species, the accuracy of the salinity reconstruction proposed here depends on numerous factors, previously listed by Berger and Gardner (1975). First is the accuracy of the

oxygen isotope measurements, which is generally better than 0.1 ‰, and which introduces an uncertainty of 0.2 in the salinity estimates. This source of error may easily be reduced by multiplying the number of measurements on foraminiferal shells. Second, we assumed that the relationship between the summer sea surface temperature and the oxygen isotopic composition of *N. pachyderma* and *G. bulloides*, determined for modern conditions, was also valid during glacial conditions. This hypothesis is clearly speculative, since glacial ecotypes may have had a different cycle due to different stratification of the water masses and a different availability of nutrients as a function of depth, which entails that environmental stresses may have differed from those in the modern ocean. *N. pachyderma* (left coiling) is the only species which lived in glacial polar waters, but several foraminiferal species live in the same waters as *G. bulloides*. They may be calibrated and used independently to estimate past sea water  $\delta^{18}\text{O}$ . The agreement between these various reconstructions will provide a test of their reliability. Third, the slope of the salinity/ $\delta^{18}\text{O}$  relationship for glacial conditions is not known and we assumed here that it was similar to the mean value for the modern climatic pattern. However, it should be stressed that the sea-water  $\delta^{18}\text{O}$  is in itself a physical parameter which characterizes the sea-water composition and is sufficient to reconstruct the surface hydrology. The accuracy of its reconstruction is not affected by our lack of knowledge of the past  $\delta^{18}\text{O}/\text{salinity}$  relationship. Salinity values are necessary only to compute density. More precise values could be derived from a realistic model of the water cycle in a glacial climate.

Last, but not least, the accuracy of the salinity estimates depends critically on the accuracy of the summer sea surface temperature estimates derived from transfer functions. In this paper, we used estimates derived from the CLIMAP (1981) reconstruction when no SST estimates were available for the glacial sediment samples. A 1°C error in SST

value would result in a 0.25 ‰ error in the calculated sea water  $\delta^{18}\text{O}$  value and a 0.5 ‰ error in the final salinity estimate. Although the reconstructions that we obtained (Fig. 7 and Fig. 9) exhibit a coherent pattern, efforts should be made to improve the reliability of the transfer functions, in particular to assess the presence of a high salinity water mass at the surface of the central part of the glacial North Atlantic Ocean.

Several conclusions can be drawn from this preliminary reconstruction. Firstly, the surface salinity distribution during the last glacial period was noticeably different from the present one. This was due to both the disappearance of the North Atlantic drift and the input of freshwater resulting from local precipitation, ice melting and river outflow. Secondly, high latitudes of the glacial North Atlantic still received a significant flux of salt, which was required to permit the formation of deep and intermediate waters. This

pattern is consistent with the presence of a small well-ventilated deep water mass which was present at the bottom of the glacial North Atlantic Ocean, north of 45°N (Duplessy *et al.*, 1988). During glacial conditions, the flux of salt from low to high latitude surface waters was, as it is today, an essential component of the global ocean circulation.

### Acknowledgements

Thanks are due to B. Le Coat and J. Antignac for help in the analysis, to N. J. Shackleton for useful discussions, and to Tom Pedersen and Lloyd Keigwin for reviewing the manuscript. This research is supported by EEC (EPOCH), PNEDC, CNRS and CEA. This is CFR contribution n° 1174.

### REFERENCES

- Aksu A. E., A. de Vernal and P. J. Mudie** (1989). High-resolution foraminiferal, palynological and stable isotopic records of Upper Pleistocene sediments from the Labrador Sea: paleoclimatic and paleoceanographic trends, in: *Proceedings of the Ocean Drilling Program, Scientific Results*, S. S. Srivastava *et al.*, editors, **105**, 617-652.
- Alvinerie J., M. Caralp, C. Latouche, J. Moyes and M. Vigneaux** (1978). Apport à la connaissance de la paléohydrologie de l'Atlantique nord-oriental pendant le Quaternaire terminal, *Oceanologica Acta*, **1**, 1, 87-98.
- Bard E., M. Arnold, P. Maurice, J. Duprat, J. Moyes and J.-C. Duplessy** (1987). Retreat velocity of the North Atlantic polar front during the last deglaciation determined by  $^{14}\text{C}$  accelerator mass spectrometry, *Nature*, **328**, 791-794.
- Bard E., R. Fairbanks, M. Arnold, P. Maurice, J. Duprat, J. Moyes and J.-C. Duplessy** (1989). Sea-level estimates during the last deglaciation based on  $\delta^{18}\text{O}$  and accelerator mass spectrometry  $^{14}\text{C}$  ages measured in *Globigerina bulloides*, *Quat. Res.*, **31**, 381-391.
- Bé A. W. H.** (1960). Ecology of recent planktonic foraminifera. Part 2: Bathymetric and seasonal distributions in the Sargasso Sea off Bermuda, *Micropaleontology*, **6**, 373-392.
- Bé A. W. H. and D. S. Tolderlund** (1971). Distribution and ecology of living planktonic foraminifera in surface waters of the Atlantic and Indian oceans, in: *Micropaleontology of the oceans*, B. M. Funell and W. R. Riedel, editors, Cambridge University Press, London, 105-149.
- Berger W. H. and J. V. Gardner** (1975). On the determination of Pleistocene temperatures from planktonic foraminifera, *J. foran. Res.*, **5**, 102-113.
- Charles C. D. and R. Fairbanks** (1990). Glacial to interglacial changes in the isotopic gradients of Southern Ocean surface water, in: *Geological history of the polar oceans: Arctic versus Antarctic*. U. Bleil and J. Thiede, editors, NATO ASI Series, vol. 308, Kluwer Academic Publishers, Dordrecht, 519-538.
- CLIMAP Project Members** (1976). The surface of the Ice-Age Earth, *Science*, **191**, 1131-1137.
- CLIMAP Project Members** (1981). Seasonal reconstructions of the earth's surface at the last glacial maximum, *Geol. Soc. Am. Map and Chart Ser.*, MC-36.
- Craig H. and L.I. Gordon** (1965). Deuterium and oxygen 18 variations in the ocean and the marine atmosphere, in: *Stable isotopes in oceanographic studies and paleotemperatures*, E. Tongiorgi, editor. CNR, Pisa, 9-130.
- Cullen J. L.** (1981). Microfossil evidence for changing salinity patterns in the Bay of Bengal over the last 20,000 years, *Palaeogeogr. Palaeoclimatol. Palaeoecol.*, **35**, 315-356.
- Duplessy J.-C.** (1970). Note préliminaire sur les variations de la composition isotopique des eaux superficielles de l'Océan Indien : la relation  $^{18}\text{O}$ -salinité. *C. r. Acad. Sci., Paris*, **271**, 1075-1078.
- Duplessy J.-C., L. Chenouard and F. Vila** (1975). Weyl's theory of glaciation supported by isotopic study of Norwegian core K 11. *Science*, **188**, 1208-1209.
- Duplessy J.-C., N. J. Shackleton, R. G. Fairbanks, L. Labeyrie, D. Oppo and N. Kallel** (1988). Deep-water source variations during the last climatic cycle and their impact on the global deep water circulation, *Palaeoceanography*, **3**, 343-360.
- Durazzi J. T.** (1981). Stable-isotope studies of planktonic foraminifera, in North Atlantic Ocean core tops. *Palaeogeogr. Palaeoclimatol. Palaeoecol.*, **33**, 157-172.
- Emiliani C.** (1955). Pleistocene temperatures. *J. Geol.*, **63**, 538-578.
- Epstein S., R. Buchsbaum, H.A. Lowenstam and H.C. Urey** (1953). Revised carbonate-water isotopic temperature scale. *Geol. Soc. Am. Bull.*, **64**, 1 315-1 325.
- Epstein S. and T. Mayeda** (1953). Variation of  $^{18}\text{O}$  content of waters from natural sources. *Geochim. cosmochim. Acta*, **4**, 213-224.
- Fairbanks R.G.** (1989). A 17,000-year glacio-eustatic sea level record: influence of glacial melting rates on the Younger Dryas event and deep-ocean circulation. *Nature*, **342**, 637-642.
- Fairbanks R.G. and P.H. Wiebe** (1980). Foraminifera and chlorophyll maximum: vertical distribution, seasonal succession, and paleoceanographic trends. *Can. J. Earth Sci.*, **17**, 831-854.
- Fillon R.H. and J.-C. Duplessy** (1980). Labrador Sea bio-, tephro-, oxygen isotopic stratigraphy and Late Quaternary paleoceanographic trends. *Can. J. Earth Sci.*, **17**, 831-854.
- Fillon R.H. and D.F. Williams** (1984). Dynamics of meltwater discharge from northern hemisphere ice sheets during the last deglaciation. *Nature*, **310**, 674-677.

- Ganssen G. and M. Sarnthein** (1983). Stable isotope composition of foraminifers: the upwelling and bottom water record of coastal upwelling, in: *Coastal upwelling: its sediment record*. J. Thiede and E. Suess, editors, NATO Conference Series, Series IV, Marine Sciences, Plenum Press, New York, 99-124.
- GEOSECS Atlantic, Pacific and Indian Ocean expeditions** (1987). Shorebased data and graphics, GEOSECS Executive Committee, H.G. Ostlund, H. Craig, S.W.S. Broecker and D. Spencer, editors, I.D.O.E., National Science Foundation, vol. 7.
- Groble H., A. Mackensen, H.W. Hubberten, V. Spiess and D.K. Fütterer** (1990). Stable isotope record and Late Quaternary sedimentation rates at the Antarctic continental margin, in: *Geological history of the polar oceans: Arctic versus Antarctic*. U. Bleil and J. Thiede, editors, NATO ASI Series, Kluwer Academic Publishers, Dordrecht, vol. 308, 539-572.
- Grousset F. and J.-C. Duplessy** (1983). Early deglaciation of the Greenland Sea during the last Glacial to Interglacial transition. *Mar. Geol.*, **52**, M11-M17.
- Hillaire-Marcel C. and A. de Vernal** (1989). Isotopic and palynological records of the late Pleistocene in eastern Canada and adjacent ocean basins. *Géogr. Phys. Quat.*, **43**, 263-290.
- Imbrie J. and N. G. Kipp** (1971). A new micropaleontological method for quantitative paleoclimatology: application to a late Pleistocene Caribbean core, in: *The late Cenozoic Glacial ages*. K.K. Turekian, editor, Yale University Press.
- Jansen E. and T. Veum** (1990). Evidence for two-step deglaciation and its impact on North Atlantic deep-water circulation. *Nature*, **343**, 612-616.
- Johannessen T.** (1987). Resente planktoniske foraminifer fra Norskehavet, Islandshavet og Nord-Atlanteren: Taksonomi, faunafordeiling og stabilisoppsammensetning. *Thesis, University of Bergen, Norway*, 2 vol., 237 pp.
- Joussaume S.** (1989). Simulation du climat du dernier maximum glaciaire à l'aide d'un modèle de circulation générale de l'atmosphère incluant une modélisation du cycle des isotopes de l'eau et des poussières d'origine désertique. *Thesis, Université de Paris, France*, 507 pp.
- Keigwin L.D. and E.A. Boyle** (1989). Late Quaternary Paleochemistry of high-latitude surface waters. *Palaeogeogr. Palaeoclimatol. Palaeoecol.*, **73**, 85-106.
- Kellogg T.B.** (1976). Late Quaternary climatic changes: evidence from deep-sea cores from Norwegian and Greenland Seas, in: *Investigation of Late Quaternary paleoceanography and paleoclimatology*, R.M. Cline and J.D. Hays, editors. *Geol. Soc. Am. Mem.*, **145**, 77-110.
- Kellogg T.B., J.-C. Duplessy and N.J. Shackleton** (1978). Planktonic foraminiferal and oxygen isotopic stratigraphy and paleoclimatology of Norwegian Sea deep-sea cores. *Boreas*, **7**, 61-73.
- Kennett J.P. and M.S. Srinivasan** (1980). Surface ultrastructural variation in *Neogloboquadrina pachyderma* (Ehrenberg): phenotype variation and phylogeny in the late Cenozoic. Cushman Foundation Special Publication n° 19, *Memorial to Orville L. Bandy*, 134-162.
- Labeyrie L.D. and J.-C. Duplessy** (1985). Changes in the oceanic  $^{13}\text{C}/^{12}\text{C}$  ratio during the last 140,000 years: high-latitude surface water records. *Palaeogeogr. Palaeoclimatol. Palaeoecol.*, **50**, 217-240.
- Labeyrie L.D., J.-C. Duplessy and P.L. Blanc** (1987). Variations in mode of formation and temperature of oceanic deep waters over the past 125,000 years. *Nature*, **327**, 477-482.
- Levitus S.** (1982). Climatological atlas of the world ocean. NOAA Professional Paper n° 13, Rockville, Maryland, USA.
- Markussen B., R. Zahn and J. Thiede** (1985). Late Quaternary sedimentation in the eastern Arctic basin: stratigraphy and depositional environment. *Palaeogeogr. Palaeoclimatol. Palaeoecol.*, **50**, 271-284.
- Mix A.C. and R.G. Fairbanks** (1985). North-Atlantic surface-ocean control of Pleistocene deep-ocean circulation. *Earth planet. Sci. Letts*, **73**, 231-243.
- Reynolds-Sautter L. and R.C. Thunell** (1989). Seasonal succession of planktonic foraminifera: results from a four-year time-series sediment trap experiment in the Northeast Pacific. *J. foram. Res.*, **19**, 253-267.
- Ruddiman W.F. and A. McIntyre** (1973). Time-transgressive deglacial retreat of polar waters from the North Atlantic. *Quat. Res.*, **3**, 117-130.
- Scott D.B., P.J. Mudie, A. de Vernal, C. Hillaire-Marcel, V. Bakij, K. D. MacKinnon, F.S. Medioli and L. Mayer** (1989). Lithostratigraphy, biostratigraphy, and stable isotope stratigraphy of cores from ODP leg 105 site surveys, Labrador Sea and Baffin bay, in: *Proceedings of the Ocean Drilling Program, Scientific Results*, S. Srivastava *et al.*, editors, **105**, 561-582.
- Shackleton N.J.** (1974). Attainment of isotopic equilibrium between ocean water and the benthonic foraminifera genus *Uvigerina*: isotopic changes in the ocean during the last glacial. *Colloque CNRS n° 219, Centre National de la Recherche Scientifique, Paris*, 203-210.
- Shackleton N.J.** (1987). Oxygen isotopes, ice volume and sea-level. *Quat. Sci. Revs*, **6**, 183-190.
- Sejrup H.P., E. Jansen, H. Erlenkeuser and H. Holtedahl** (1984). New faunal and isotopic evidence on the late Weichselian-Holocene oceanographic changes in the Norwegian Sea. *Quat. Res.*, **21**, 74-84.
- Thunell R.C. and S. Honjo** (1987). Seasonal and interannual changes in planktonic foraminiferal production in the North Pacific. *Nature*, **328**, 335-337.
- Veum T.** (1990). Sen Weichsel Paleoseanografi og paleoklima i Norskehavet og Nord Atlanteren. *Thesis, University of Bergen, Norway*, 171 pp.
- Vogelsang E.** (1990). Paläo-Ozeanographie des europäischen Nordmeeres an Hand stabiler Kohlenstoff-und Sauerstoffisotope. *Thesis, University of Kiel, Germany*, 207 pp.
- Wefer G., G. Fischer, D. Fuetterer and R. Gersonde** (1988). Seasonal particle flux in the Bransfield strait, Antarctica. *Deep-Sea Res.*, **35**, 891-898.
- Wefer G., E. Suess, W. Balzer, G. Liebezeit, P. Muller, C.A. Ungerer and W. Zenk** (1987). Fluxes of biogenic components from sediment trap deployment in circumpolar waters of the Drake Passage. *Nature*, **299**, 145-147.
- Williams D.F., A.W.H. Bé and R.G. Fairbanks** (1981). Seasonal stable isotopic variations in living foraminifera of the Indian Ocean. *Palaeogeogr. Palaeoclimatol. Palaeoecol.*, **33**, 71-102.
- Zahn R.** (1986). Spätquartäre Entwicklung von Küstenauftrieb und Tiefenwasserzirkulation in Nordost-Atlantik. Rekonstruktion anhand stabiler Isotope kalkschaliger Foraminiferen. *Ph. D. Thesis, University of Kiel, Germany*